

Article

Supercapacitors in Tandem with Batteries to Prolong the Range of UGV Systems

Namin Shah *  and Dariusz Czarkowski

Danamio Research Facility, 7 Imperial Court, Monroe Township, NJ 08831, USA; dc1677@nyu.edu

* Correspondence: nshahschoolemail@gmail.com

Received: 2 December 2017; Accepted: 4 January 2018; Published: 10 January 2018

Abstract: The purpose of this study was to explore a novel approach to power hybridization in relation to its effectiveness in an unmanned ground vehicle (UGV). This hybridization method is modeled after the power distribution methods found in living organisms, which utilize glycogen stores and adipose tissue to optimize power and energy density strengths and weaknesses. A UGV rover was constructed with an appropriate distribution of power storage elements creating separate power buffers. The primary buffer consisted of a 10 W solar panel array and a 600 F, 5.4 V supercapacitor bank, and the secondary buffer consisted of a 3.7 V 6 Ah lithium-ion battery pack. The primary buffer provided virtually limitless charge cycles with a superior power density juxtaposed with a secondary buffer that provided superior energy density and volumetric versatility. The design of this rover is presented in this paper; it was tested under manual and autonomous modes. The rover was found to be capable of effectively operating solely on the primary power buffer in high to low luminous conditions while being able to carry out basic extravehicular activities. The rover could travel roughly 22 km without any input power on a full charge of both buffers, and could smoothly switch between its own power buffers during operation, all while transmitting live first person video (FPV) and network data. The introduction of control algorithms on the onboard microcontroller unit (MCU) was also explored in both manual and autonomous configurations. The latter integrated linear regression to intelligently manage power and locomotion based on sensory data from photoresistors.

Keywords: supercapacitors; hybridization; rover; machine-learning; perturb-and-observe; solar; lithium-ion; Internet-of-Things; exploration; unmanned-ground-vehicle

1. Introduction

The proliferation of electronic and robotic systems including electric cars, drones, and rovers continues to sweep the globe. Due to advances in the software, cost, and functionality of these devices, their power demands have subsequently increased leading to a rather large dependence on traditional portable power systems. These power systems have also grown and have been adapted to fit the needs of these devices. Today, most of these devices utilize power storage systems containing a single power buffer consisting of electrochemical cells in the form of batteries. Lithium-ion and lithium-polymer batteries are the most common of these systems [1], as opposed to nickel-cadmium and lead-acid batteries, which seldom see use in an unmanned ground vehicle (UGV) and electric vehicle (EV) systems due to their inferior energy densities and/or costs [1]. All of these battery systems have seen advancements in their cost, energy density, and relative safety. Electrochemical cells remain among the most volumetric and energy efficient power systems for applications in unmanned aerial vehicles (UAV), unmanned ground vehicles (UGV) [2], and in full-sized electric cars [1]. However, these power systems still contain weaknesses that create limitations for the devices that they power. Other power storage systems such as traditional capacitors and flywheels contain very little usable energy relative to their size and are useful in supplementary roles for only fringe applications. On the other hand,

a supercapacitor (SC) still contains relatively inferior volumetric and energy densities (in relation to batteries), along with greater costs [3–5], but has large power densities and increased versatility that balance some of the downfalls of battery systems. Supercapacitors are too large for use in UAVs and cannot meet the full energy demands of full-sized electric vehicles. However, a method of hybridizing batteries and SCs can be implemented in a UGV system. The number of charge cycles that an SC can handle is directly proportional to its effective lifespan on a UGV system equipped with solar cells tasked with constantly recharging the power storage system. Lithium-ion (Li-ion) or any other battery system falls short on this front and fails to survive for even a fraction of the charge cycles of a typical supercapacitor [6]. Upon these limitations, it becomes clear that a UGV device equipped with a hybrid power system must be designed to operate primarily through the use of SCs and with Li-ion cells acting in a supplementary manner to provide power for activities that are required during energy scarcity. As a result, the bulk of the charge cycles will fall on a sole SC power bank, eliminating the need for active cooling systems and multiplying the lifecycle of the Li-ion power bank [6]. A UGV system capable of utilizing both SCs and Li-ion cells similarly to the way the human body uses glycogen and fat stores was tested. The power system utilizes a connected microcontroller to implement an algorithm designed to mimic the energy processes of the human body. Quick, easy to use bursts of energy are primarily relied upon as glycogen constitutes the majority of human energy consumption, making it a primary power buffer. At the same time, any excess energy is stored in a slow to use yet volumetric and energy-superior power storage system, similar to ectopic fat in adipose tissue acting as a secondary power buffer. Implementing such a system in a UGV would most importantly drastically improve the number of charge cycles that the device can undergo while retaining a plethora of the benefits of a traditional SC battery hybrid system. If used in junction with Li-ion batteries in proper proportion coupled with an intelligent algorithm, the integration of an SC power buffer can drastically improve the lifespan and functionality of a scale solar UGV system. The increased longevity of a UGV system can have significant applications. By utilizing the nearly infinite number of charge cycles in order to perform without deterioration, UGV rovers can be used to explore areas far from places that are traditionally accessible. Uses include search and rescue systems and even a low-cost alternative for space rovers. The power distribution method can also be applied to other devices capable of mechanical motion such as cloud-connected aquatic robots capable of reporting current and weather that for many years use the sun and water currents, with the help of SCs, for power. In this paper, the design and implementation of a novel approach to SC Li-ion hybridization are presented in relation to their effectiveness in a cloud-connected rover. This approach utilized a cloud-connected microcontroller with relays and transistors to switch between power buffers. By doing so, the rover presented in this paper possesses the ability to drive for vast distances without exhausting the finite charge cycles of the traditional battery systems.

2. Methodology

2.1. A. Initial Build and Power System Configurations

A 10 W solar panel array provides the entirety of the input power due to its abundance and previously successful implementation in exploratory applications [2]. As is the nature of solar energy, be it here on Earth or another planetary surface, the availability of sunlight can vary dramatically due to many factors such as the time of day, weather patterns, and environmental interference of the panels (i.e., dust, dirt). However, in any given environment, the position of the rover may be changed to increase the input energy (see Section 2.4 for solution). Under direct sunlight, the input power would exceed the storage capacity of the primary power buffer (SC bank). However, since the rover is intended to be constantly active and usable, the excess power is distributed amongst ongoing operations and the lithium-ion bank as needed. The SC bank exists to operate the rover during periods of shade and or when the rover has navigated into locations of temporary shade. Thus, the rover containing both an SC and a Li-ion system was built and ultimately used for collecting power statistics.

2.2. B. Rover Design Specifications

A 4-motor chassis was used as the base for the hardware of the rover. This chassis consisted of four individual brushed DC motors. The motors were connected to the drive wheels in a 1:120 gear ratio. This setup allows for sufficient torque to carry the load of two separate power systems. The entire rover weighed 2.25 kg. Table 1 provides the weight distribution of the rover. In order to model the energy system that is present in living organisms, a substantial power store was required. This store was split between an SC bank and a Li-ion battery pack. The rover was tested in several stages with different setups and configurations regarding its hardware and software. Initially, the rover was fitted with six 2.7 V 400 F supercapacitors wired in series-parallel to create a 5.4 V 600 F supercapacitor bank. As per the dimensions of the motor chassis, six was a reasonable number of supercapacitors that could volumetrically fit on the rover. An additional six 3.7 V 18,650 lithium-ion batteries were wired to create an 11.1 V lithium-ion battery pack. The Particle Photon was used as the MCU for the rover allowing for internet connectivity for data reporting. The voltage of the panels, SC bank, and Li-ion pack were measured using voltage dividers fed into the board's analog to digital converter (ADC) pins. The live-current draw of the rover was more of a challenge and required the use of a modified A1302 analog magnetic Hall effect sensor fitted with a toroidal coil wrapped in magnet wire creating an inductor coil, which was wired in series with the power input of the rover and the primary power buffer. As the magnetic field is generated by current flow $B_{center} = \mu_0 I / (2a)$, the Hall effect sensor provides an analog value proportional the B value. It had to be calibrated to report current accurately in amperes and is shown in Figure 1 and Table 2. While the rover was operating, both voltage and current data were reported live to a Ubidots web server via the cloud connection. The system was designed to operate both autonomously and controlled in order to increase the versatility of the rover. Testing was done under both operating systems to validate the effectiveness of the algorithm designed to seek out and manage power use, as opposed to manual control. Considering that the aim was to also demonstrate the effectiveness of supercapacitors as the primary power buffer for a motorized mobile electronic system, the manual tests are equally valid. The manual control was done using an external RC module with a corresponding drive controller. The transition between power buffers remained autonomous through every test and configuration as the ADC reads merely for a threshold low in the SC and panel voltage to trigger the onboard relay to switch to the secondary power buffer.

Table 1. Weight and weight distribution of the rover.

Apparatus	Weight in Grams (g)
Panel array	405
Lithium-Ion battery pack	305
Supercapacitor bank	434
Motors/chassis	660
Circuit/breadboard/wires	196
Total weight of rover	2000

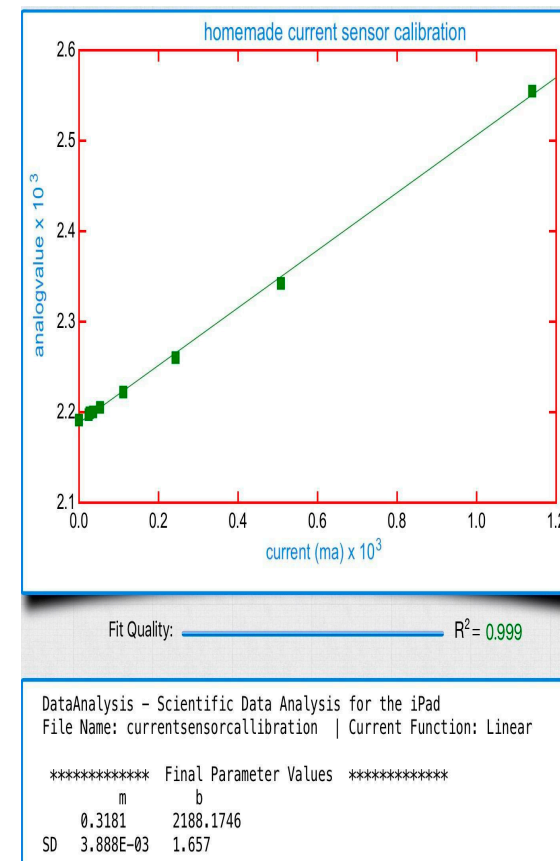


Figure 1. Graph of data with m value of 0.3181.

Table 2. Hall magnetic sensor data from different loads.

Load Resistance (Ohms)	Raw Analog In (Average of Two Values Received)	Measured Current (Milliamps)
220	2297.5	24.3
200	2199.5	26.8
150	2200.5	35.7
100	2205.5	53.1
47	2222.5	111.5
22	2260.5	243.0
10	2342.5	508.0
DC motor	2555.0	1140.0
No load	2192.5	0.0

2.3. C. Longevity Test

Utilizing an SC bank as the primary power buffer of the wireless rover provides, most importantly, an extended number of charge cycles allowing the rover to stay on and usable for extended periods of time without human intervention. To determine the effective lifespan of the rover, tests were completed in different sunlight conditions to determine the distance that the rover could travel. The goal is to create a rover with a power system capable of allowing the rover to drive continuously while relying only on the irregular windows of sunlight available. The first test to help quantize the designed rover’s abilities was a raw distance test. For this test, the intent was to measure the amount of energy required to move the rover a specific distance. By essentially calculating the force produced by the rover, the internal energy stored in each of the buffers could be used to determine how many meters the rover could travel using that stored energy. This test was executed on a flat surface of 3 m with the rover under manual control. An external microcontroller circuit with a laser diode and a laser light sensor was used to measure an accurate time for the rover. This time was used to approximate the Integral

$\int_a^b \text{current } dx$, which yields the total charge in coulombs. This value combined with the average voltage during each test provided the energy in joules by $E = QV$. During each test, the rover was manually driven across the 3 m surface in a straight line and voltage measurements were made before and after each test to determine the average voltage. The rover itself transmitted live current values (see Figure 1). The average velocity of the rover was measured and recorded during each test.

2.4. D. Power Algorithm for Autonomy

The rover was equipped with an algorithm designed to actively ‘seek out’ power in any given environment. This was done to emulate the power distribution characteristics of aerobic life. Essentially, the rover can maneuver in order to increase the amount of direct sunlight making contact with the rover, thereby increasing the total power available from the panels. Such maneuvers would have to evaluate sensory data and account for predicted power expenditure in order to decide what maneuvers if any would net increase the rover’s input power. The autonomous mode integrates a simple linear regression algorithm that evaluates data from two photoresistors (located far along on each edge of the rover’s panel surface (see Table 1 and Figure 2). Since photoresistor values are highly prone to variance due to numerous environmental factors specific to each particular time, place, and position of the rover, the algorithm had to account for these variances on a trial by trial basis. Therefore, the regression algorithm was used to predict if motion in either direction would increase the panel voltage. The rover was ‘rewarded’ if the panel voltage did in fact increase and if the total power expended in each maneuver was less than the power gained from the maneuver [7]. Specifically, the algorithm measured raw sensor values from the front and back. Using these values, a prediction would be made using an array of previously attained values and the correlation with power increased. This mechanism allows the rover to adapt to new environments and continue to make maneuvers to increase the available power, thus increasing the usable energy when manual use is needed. Initially, the software did little to improve power. However, the idea behind using a machine learning algorithm is that after some ‘experience’ the rover would act to implement power optimization, a form of maximum power point tracking (mppt) using perturb and observe analysis: the rover perturbing in a direction and observing the resulting power level to predict when and where to move.

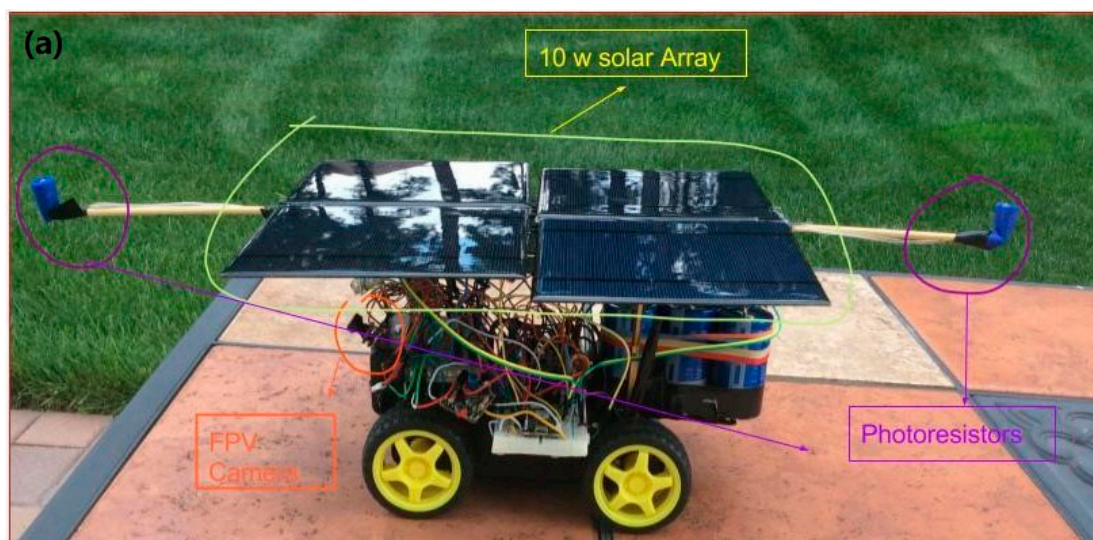


Figure 2. Cont.

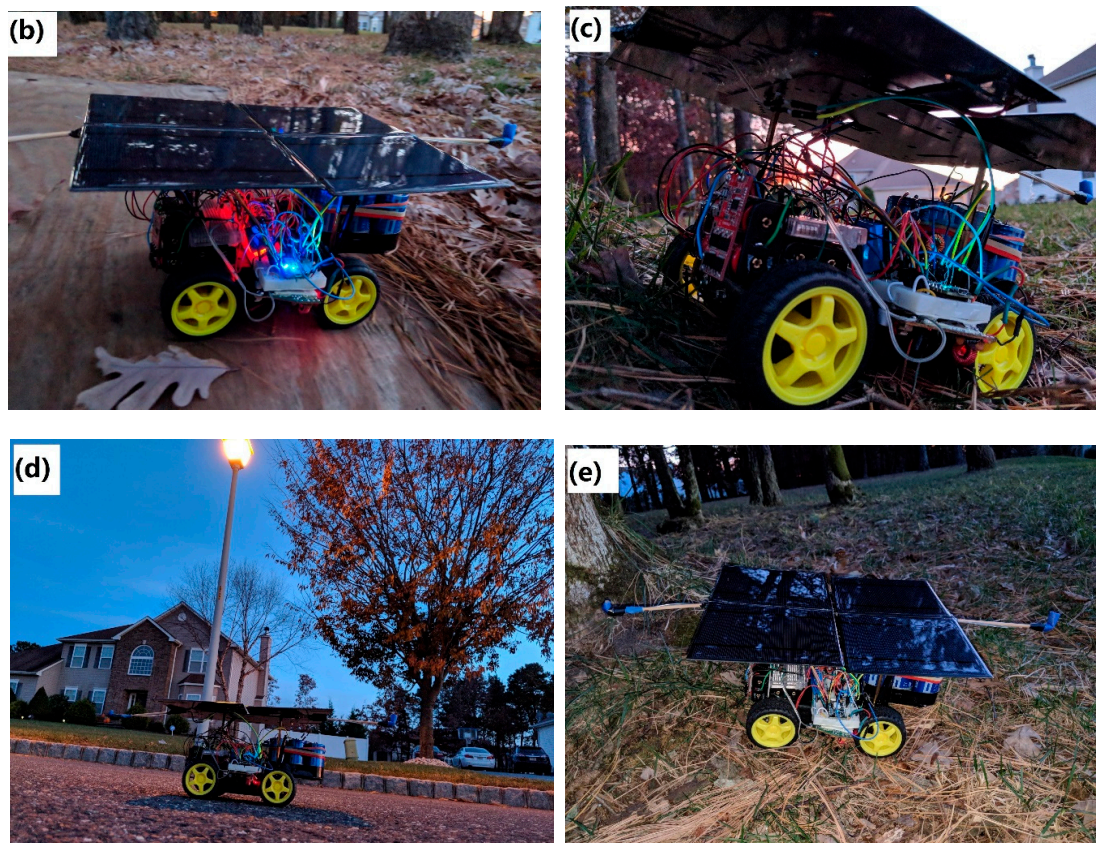


Figure 2. Rover hardware and design. Circuitry containing RC receiver and motor driver. (a–e) Circuitry containing Particle Photon board, voltage divider for voltage measurements, toroid coil to centralize magnetic field associated with Hall sensor, balance board to power MCU, power switch relay, and battery management system for Li-ions. Overall pictures of Rover size and environmental application.

3. Results

The rover functioned as designed for most intended extravehicular functions. In this case, the rover's power buffers were powering the drive of the rover, the radio controlled (RC) receiver, and a 25 mW FPV camera that transmitted live video during the tests. The primary buffer handled all of the loads sufficiently. The ADC successfully transmitted live voltage data and the Hall effect sensor transmitted live current data to a Ubidots host server where the data was stored. Figure 1 shows the Hall effect calibration from raw analog values to an input measuring current in amperes. A conversion formula was developed and embedded in the software of the rover. The computation was done with data using the data analysis tools of the Ubidots service [8]. During testing, the software displayed a live chart displaying current draw and the panel/SC bank voltage. Since the solar array was connected in parallel to the SC bank, the reported voltage was reflective of increases in sunlight exposure along with excess power usage.

The total weight distribution of the rover can be seen in Table 1. The testing of the rover was conducted on a flat concrete surface with minimal bumps and slopes. On this platform, the rover performed effectively handling the power demands both of the given extravehicular activities of full 360 locomotion and live FPV video. Since the four individual motors of the rover were paired off and wired in parallel, the right motors operated as one unit and the left motors operated as one unit. For both manual and autonomous tests, the current draw varied tremendously. During the manual tests, the current draw of the motor driver board fluctuated around 1 A during full forward motion. During half turns, the rover would engage only one side of motors and pivot around stationary

wheels. Under a full duty cycle half turn, the current draw would approach 1.2 A. While completing a full turn the rover would spin each side of motors in opposite directions and a full duty cycle full turn would draw the most current at around 1.4 A–1.6 A, depending on the voltage of the power buffers. At lower voltages (less than 4.0 V), the rover would not be able to complete full turns at a practical speed and would resort to only half turns. The variance in the current draw created new design challenges. Mainly, the transition device from the primary to secondary power buffer became a 5 V/10 A electromechanical relay controlled by a bipolar junction transistor (BJT) as opposed to the transistor alone. The relay provides a direct path for the current to flow without a risk of overheating and accidental shorts. Another challenge that arose was that of the input voltage source of the motor driver. The secondary primary buffer configured in an 11.1 V, three series battery configuration drove the rover with more power at any given instant as the current values measured were roughly equivalent if not greater than that of lower voltages. As a result, the rover would move faster with more power. In order to make the voltage of the capacitors higher, a voltage boost module was used; however, it responded poorly to the fluctuating current draw and would stall and prevent the motors from drawing the necessary current. The direct connection between the SC bank and the motor driver input ended up being the most effective option with no current restrictions.

The input path of the primary buffer follows the closed path of the relay, while the secondary buffer is interrupted by the open path. A digital high signal to the control transistor of the relay closes the secondary path and opens the primary path. This system worked effectively and the rover was essentially able to switch its own power source. In order to accomplish this, the Photon MCU had to hold a reference voltage from the secondary buffer at all times. The reference allows for accurate voltage measurements of the primary buffer and allows the rover to make the switch between buffers. Testing of voltage measurements without the reference voltage made for erratic and inaccurate voltage readings. Considering that the Photon drew only around 60 mA when it was on and operating fully and only 3 mA when in sleep mode, the load of the MCU will likely never place any significant strain on the 6 Ah secondary buffer. However, the MCU is still also powered by the primary buffer through its voltage input VIN pin to further remove strain on the secondary buffer.

The rover's usability depends on the distance that it can travel with and without sunlight. The following tests demonstrate this ability in depth. Figure 3 shows the raw distance test results of the rover. The average values for the ten individual trials were used in the energy distance calculations.

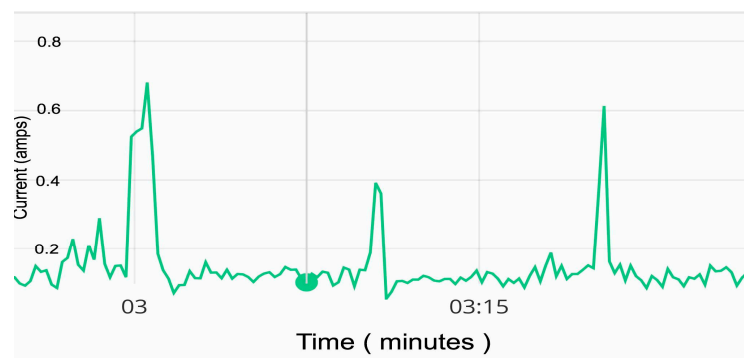


Figure 3. Raw distance tests 1–3 of current over time. $\int_a^b \text{current } dt$ represents total charge where $b - a =$ measured time. Spikes roughly represent exact time spans when the rover was in motion.

Average time: 20.0776 s. Average voltage: 4.965 V.

Average charge (see Table 3 for graph): 7.3115 coulombs. Distance: 3 m.

$$E = QV = 7.3115 \text{ Q} \times 4.965 \text{ V} = 36.6 \text{ J} \quad (1)$$

$$F = \frac{36.6 \text{ J}}{3 \text{ m}} = 12.1 \text{ N} \quad (2)$$

Cap voltage when fully charged: 5.4 V at 600 F. At roughly 3.0 V the rover can no longer move.

$$\frac{1}{2}CV^2 = \frac{1}{2} \times 600 \times 5.42 = 8748 \text{ J} \rightarrow \frac{1}{2} \times 600 \times 3.02 = 2700 \text{ J} \quad (3)$$

$$8748 - 2700 = 6048 \text{ J} / 12.1 \text{ N} = 499.8 \text{ m} \quad (4)$$

This means that under circumstances of no light, the rover can move a distance of about 0.5 km just with power from the SC bank. The average velocity during these tests was 0.149 m/s. An extension of this calculation to account for the full power capacity of the rover includes calculating the energy capacity of the secondary power buffer, the Li-ion batteries.

Table 3. Raw distance test results.

Trial #	Time (Seconds)	Start Voltage (V)	End Voltage (V)	Total Charge (Coulombs)
1	15.720	5.23	5.20	8.105
2	16.468	5.12	5.10	5.703
3	17.298	5.09	5.06	7.410
4	18.961	5.04	5.01	6.133
5	19.764	5.00	4.96	6.811
7	22.123	4.90	4.87	7.803
8	22.280	4.86	4.84	8.061
9	23.119	4.82	4.79	6.980
10	24.920	4.77	4.75	9.201
Avg	20.078	4.98	4.95	7.3115

The charged voltage of the Li-ion batteries is 12 V. The total capacity is 6 amp hours.

$$6 \text{ Ah} \times \frac{3600 \text{ s}}{1 \text{ h}} = 21,600 \text{ A} \cdot \text{s} \quad (5)$$

$$21,600 \text{ A} \cdot \text{s} \cdot \frac{1 \text{ C}}{1 \text{ A} \cdot \text{s}} = 21,600 \text{ C} \quad (6)$$

$$P_{\text{elec}} = qV = 21,600 \text{ C} \times 12 \text{ V} = 259,200 \text{ J} \quad (7)$$

$$259,200 = 259,200 \text{ Nm} \times \frac{1}{12.1 \text{ N}} = 21,421.5 \text{ M} = 21.42 \text{ km} \quad (8)$$

The total sum of travel without any exposure to sunlight was about 21.9 km.

The three main sunlight conditions were full sunlight, clouded evening, and nighttime. During full daylight, the rover received the full 10 watts of power from the sun and could drive at full speed, make turns, and carry out various extravehicular maneuvers without decreasing the voltage of the motors. Figure 4 shows the voltage of the primary buffer and the current draw of the rover during testing done during bright direct sunlight. It can be noticed that the primary buffer voltage continued to increase when the current draw was high. Specifically during the full duration of the test, $\int_{15:55}^{16:20} \text{Current } d(t) = 388.08 \text{ C}$ while $\Delta V = +0.74 \text{ V}$. This increase, despite losing charge to the motors, is duly noted. When the rover was tested again during clouded evening conditions during the time of sunset, different results were achieved. The primary buffer voltage remained roughly constant during periods of a minimal current draw and would barely dip when the rover was moved, as seen in Figure 5. However, perhaps most astonishing is the fact that the voltage levels increased after the rover was manually re-positioned to an area with more direct sunlight. At the time mark of 20:07 in Figure 5, the rover moved and as the sun began to set the primary buffer continued to gain voltage due to the adjustment. This uptick was due to the nearly zero current draw and improved position of the rover. As soon as the sun set entirely, the board experienced a brief internet disconnection. The voltage under pitch darkness dropped dramatically, as expected. The results of this test provide support for the need of an intelligent algorithm to maximize the rover's power availability. Another test was completed in

sunset conditions and is displayed in Figure 6. This test corroborates the path from Figure 4 during the evening luminous conditions; that being a standard almost linear voltage level even during small movements. These outdoor tests express that the rover can gain energy from the panels during the evening hours approaching darkness.

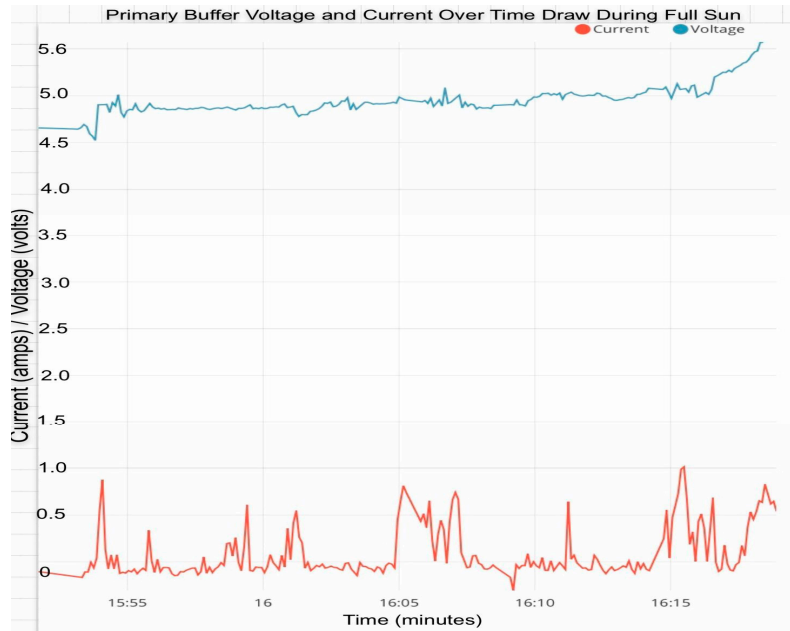


Figure 4. Rover outdoor test under direct sunlight.

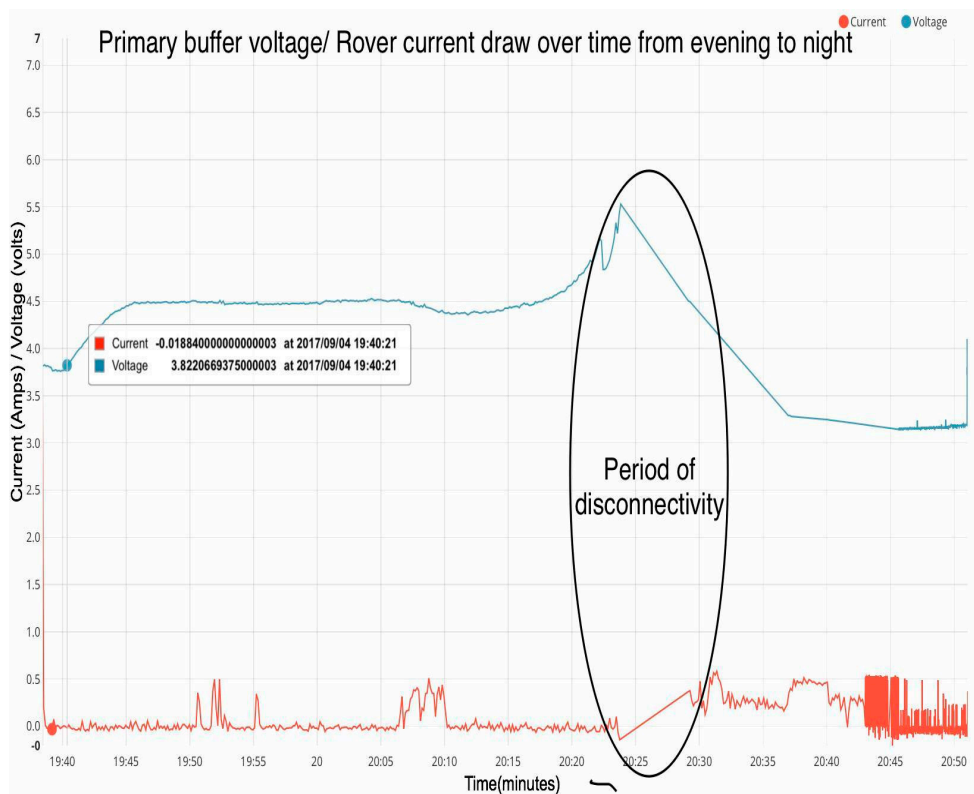


Figure 5. Rover outdoor test during evening hours from sunset into the night.

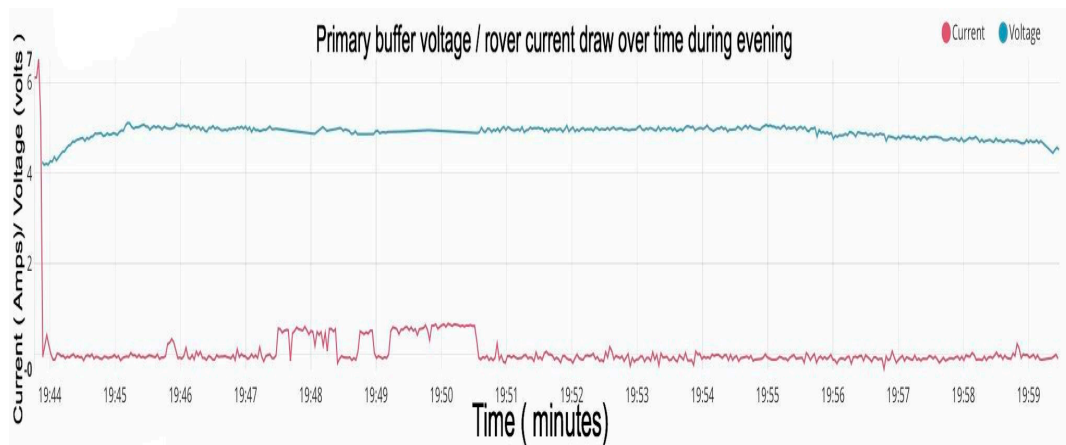


Figure 6. Second test during lower luminous intensity. Voltage dips slightly during current spikes. The voltage increases very slowly during rest periods.

Direct, cloud-free sunlight conditions provide the rover with sufficient power so as to prevent the necessity for the use of the secondary buffer. However, during all other conditions, the rover has to be operated accordingly in order to prevent usage of the secondary buffer. A novel approach was taken to create a ‘mode’ for the rover in which the rover only acts to gain power. Two photoresistors were added past either side of the rover’s panel array. The analog data coming from these resistors were used in a regression algorithm where the rover would predict a ‘reward’ for an action and act upon actions with the most predicted rewards. The rover would be ‘rewarded’ if the primary buffer increased in voltage and was ‘punished’ if the opposite was true. The results of testing this algorithm were actually beneficial. At first, the rover would continuously make actions such as moving backward or forward, which cost more energy than was gained. However, after a while of being placed out, the rover began to consistently choose the direction with the higher photoresistor reading, depending on the magnitude of both. The rover would stay still if both readings were roughly equal (see Figure 2 for hardware setup).

4. Discussion

The power density, quick charge time, and ease of use of supercapacitors have made them the subject of extensive experimentation for their potential to be implemented alongside battery systems. In the case of motorized devices, they have found success in electric vehicles to efficiently capture brake regeneration voltage to balancing the power demands with energy demands [3]. Traditional hybridization methods previously tested on robotic devices have focused on using SCs as supplements for the battery system. Previous research consists mainly of additive compositions of SCs and Li-ions where SCs handle high current operations providing short bursts of power (i.e., getting a rover or car up to speed or instantaneous momentum shifts) while the battery systems remain the primary power system onboard [9]. They perform well and improve the duration of these vehicles by improving power input efficiency (i.e., regenerative braking); however, they do not dramatically alter the longevity of the vehicle. In this paper, the SC bank acted as the primary energy source for the rover. Smaller-scaled unmanned ground vehicles (UGVs) contain far lower power to weight demands for functionality and standard operation than electric cars and can easily be fitted with solar cells of sufficient surface area to meet power recharge demands. Panels cannot easily be used in full-sized electric vehicles due to lack of surface area and increased bulk/inconvenience. This smaller demand can allow for a primary buffer consisting of entirely SCs. As described earlier, a UGV with these characteristics can act much like living organisms that undergo cellular respiration. The ongoing analogy of SCs to glycogen and Li-ion to adipose tissue is alarmingly accurate. Designing and testing a rover implementing such a system was the focus of this study and has never been examined before. In studies that explore its application

in stationary sensor power management systems, this method of hybridization has been shown to dramatically prolong lifetimes [6,9]. The objective of this paper was to extend this idea onto a moving device capable of performing extravehicular tasks. This would mean that new practical uses for the combination of these technologies can be achieved, including tasks to improve power availability that lead to interesting software algorithms which can further improve lifespan. Weight and surface area variables along with environmental responsivity and more substantial power demands represent some of the additional challenges that come about in building a rover. The device built in this paper could hypothetically, if protected adequately from physical weather elements, drive across a country while undergoing thousands of charge cycles. The fact that the device has the ability to move unlike a sensor network [6] or a wind turbine monitor [10] means that the addition of neural networks to establish simple to complex machine learning algorithms can further improve usability. As was briefly explored in this paper, smart algorithms can intelligently be used to further prolong the life of hybrid electric vehicles [4]. The usage of more complex neural networks was explored successfully [11] and can be used to improve or prolong the lifespan of a hybridized UGV.

5. Conclusions

After the complete development of the rover, the results corroborate the idea that a device with similar specifications could remotely or autonomously traverse vast distances. It may do so over an extended period through many recharge cycles. A UGV system to implement this particular style of hybridization would endure significantly more charge cycles by balancing power distribution across two power buffers. The idea of SC hybridization has been experimented thoroughly and has yielded positive results. However, this method of hybridization remains mostly unexplored especially in a UGV system. The versatile abilities of a moving device provides unique opportunities for power maneuvers as opposed to stationary sensors and devices. The end goal of this study was to create a practical and usable device as much as it was to explore the possibilities of different power systems. In that regard, the study was successful. The final device can efficiently drive and can serve a practical purpose. A working system was built and presented that functioned more or less how it was anticipated to. The rover built in this study demonstrates one possible distribution for this sort of hybridization when in reality there exist a large number of weight, power, and energy combinations for the SC bank, the Li-ion pack, and the rover's size and power requirements. Perhaps the most important extension of this study would be to test different combinations of these systems to determine which size and capacity of SCs and batteries would work most efficiently. Also, as was narrowly explored in this paper, the integration of machine learning into the management of UGV and UAV power systems is intriguing and worth exploring down the line.

Author Contributions: Namin Shah conceived and designed the experiments along with rover construction; Namin Shah performed the experiments; Namin Shah and Dariusz Czarkowski analyzed the data; Namin Shah wrote the paper; Dariusz Czarkowski contributed experimental advice and paper revisions.

Conflicts of Interest: The authors declare no conflict of interest.

References

1. Lokhande, S. Batteries Used in Electric Vehicles. *Int. J. Technol. Res. Eng.* **2016**, *4*–16.
2. Ratnakumar, B.V.; Smart, M.C.; Whitcanack, L.D.; Ewell, R.C.; Surampudi, S. *Li-Ion Rechargeable Batteries on Mars Exploration Rovers*; Jet Propulsion Laboratory, California Institute of Technology: Pasadena, CA, USA, 2004. Available online: <http://citeseerx.ist.psu.edu/viewdoc/download?doi=10.1.1.606.8642&rep=rep1&type=pdf> (accessed on 15 August 2017).
3. Chau, K.T.; Wong, Y.S. Overview of power management in hybrid electric vehicles. *Energy Convers. Manag.* **2002**, *43*, 1953–1968. [[CrossRef](#)]
4. Drosos, C.; Vernardou, D. Perspectives of energy materials grown by APCVD. *Sol. Energy Mater. Sol. Cells* **2015**, *140*, 1–8. [[CrossRef](#)]

5. Vernardou, D. State-of-the-art of chemically grown vanadium pentoxide nanostructures with enhanced electrochemical properties. *Adv. Mater. Lett.* **2013**, *4*, 798–810.
6. Jiang, X.; Polastre, J.; Culler, D. Perpetual environmentally powered sensor networks. In Proceedings of the 4th International Symposium on Information Processing in Sensor Networks (IPSN), Boise, ID, USA, 15 August 2017; pp. 463–468. [[CrossRef](#)]
7. Shah, Namin Github Source Code for Rover by Namin Shah. Available online: <https://github.com/NaminShah/Supercapacitor-rover> (accessed on 27 September 2017).
8. Pay, S.; Baghzouz, Y. Effectiveness of battery-supercapacitor combination in electric vehicles. In Proceedings of the 2003 IEEE Bologna Power Tech Conference Proceedings, Bologna, Italy, 23–26 June 2003; Volume 3, p. 6. [[CrossRef](#)]
9. Li, W.; Joos, G. A power electronic interface for a battery supercapacitor hybrid energy storage system for wind applications. In Proceedings of the 2008 IEEE Power Electronics Specialists Conference, Rhodes, Greece, 15–19 June 2008; pp. 1762–1768. [[CrossRef](#)]
10. Moreno, J.; Ortúzar, M.E.; Dixon, J.W.; Member, S. Energy-Management System for a Hybrid Electric Vehicle, Using Ultracapacitors and Neural Networks. *IEEE Trans. Ind. Electron.* **2006**, *53*, 614–623. [[CrossRef](#)]
11. Ubidots Iot Web Host. Available online: <https://ubidots.com/> (accessed on 9 September 2017).



© 2018 by the authors. Licensee MDPI, Basel, Switzerland. This article is an open access article distributed under the terms and conditions of the Creative Commons Attribution (CC BY) license (<http://creativecommons.org/licenses/by/4.0/>).